ISSN: 2692-5397
DOI: 10.33552/MCMS.2023.05.000609
Modern Concepts in Material Science
Iris Publishers

Research Article

Effect of Micro-Arc Oxidation Voltage on the Morphology and Electrochemical Properties of AZ31B Magnesium Alloy

Ameeq Farooq[1], Ahsan Saleem[1], Kaab Bin Tayyab[1], Hafiz Muhammad Rehan Tariq[2], Hafiz Waqar Ahmad[3], Umer Masood Chaudryb[2,4]* and Tea Sung Junb[2,4]*

[1]*Institute of Metallurgy & Materials Engineering, University of the Punjab, Pakistan*

[2]*Department of Mechanical Engineering, Incheon National University, Republic of Korea*

[3]*School of Mechanical Engineering, Sungjyunkwan University, Republic of Korea*

[4]*Research Institute for Engineering and Technology, Incheon National University, Republic of Korea*

***Corresponding author:** Umer Masood Chaudry and Tea Sung Jun, Department of Mechanical Engineering and Research Institute for Engineering and Technology, Incheon National University, Incheon 22012, Republic of Korea.

Received Date: June 09, 2023

Published Date: June 19, 2023

Abstract

In this research work micro arc oxidation (MAO) is used to modify the AZ31B magnesium alloy surface to improve the degradation and corrosion properties in the simulated body fluid. Optimum voltages of 125 V, 200 V and 250 V were selected for MAO in sodium silicates, sodium fluoride and borax solution. The resulting surface modification was observed by stereomicroscope and Scanning Electron Microscope. Modified surface stability and corrosion resistance were also assessed in simulated body fluid i.e., Ringer's Lactate at 37 ± 1 °C with open circuit potential and cyclic polarization. Results showed more uniform and stable MAO coating was obtained at 200 V which shows corrosion resistant than the other two coatings.

Keywords: Magnesium, Microarc-oxidation; Cyclic polarization; Ringer's lactate

Introduction

Magnesium and its alloys are recognized as ultimate suited and lightest metallic material for structural and industrial applications because of its novel properties as high strength to weight ratio, recyclability, high thermal conductivity and good machinability [1]. Because of their conventional applications magnesium and its alloys stand out in automobile industry, electronic devices and in biodegradable implants as they are nontoxic and biodegradable in body environment [2,3]. Due to high reactivity of magnesium, it is susceptible to undergo corrosion reaction and develops an unstable oxide layer hence unable to provide protection to its surface [4].

As a result of interaction with dissimilar metals acquiring electrochemical potential in ionic path, magnesium acts as an anode at high potential as it is highly active metal and promote galvanic corrosion [5,6]. Intergranular corrosion (IGC) at grain boundaries is another form of corrosion in contrast to pitting because it is crucial to identify surface pits due to corrosion products [7,8]. Acute localized dissolution to metal matrix takes place due to these corrosive pits i.e., pitting is very crucial in orthopedic applications as it enhances corrosion and propagates cracks [9]. Evolving hydrogen due to corrosion and causes balloon effect when absorbed in vivo condition [10]. There are various approaches to enhance the biocompatibility and corrosion resistance i.e., adding different alloying elements, developing biocompatible, protective and corrosion resistance coatings [11]. Surface modification is a well-known technique to carry out different challenges associated with metallic implants in the highly corrosive environment i.e., human body and for enhancement of implants related to corrosion behavior [12]. Utilization of biomedical coatings [13], Micro-arc oxidation coating (MAO) / Plasma electrolytic oxidation (PEO) [14,15], calcium phosphate coatings [16], organic coatings [17], oxide layer development, surface texturing and ion beam processing [18]. Inorganic coatings offer surprising resistant properties, still they have limitations i.e., high temperatures for densification [19,20]. Densification of organ-

ic and inorganic coatings usually develops at low temperature (300 °C) which permits the achievement of glassy structures without crystallization and altering the microstructure of magnesium alloys [21,22]. Micro-arc oxidation (MAO) has been generally utilized to develop strong and porous coatings on magnesium and its alloys and then widely used as improved corrosion resistant implants. MAO is a surface engineering method that shows the capacity to improve the adhesion of conclusive top-coat [23,24]. MAO coatings on magnesium have tri-layer structure. The top layer consists of deep pores and cavities having a permeable nature, middle layer is less porous layer, and the bottom layer is a thin obstruction layer. To attain high bond strength and enhance mechanical properties, these pores are advantageous as they release the residual stresses. Distribution of pores, pore density and pore structure are the major aspects that determine the capacity of coating to resist corrosion [25-27]. During MAO of magnesium alloys the nature and concentration of the alloying elements, applied voltage or current, type of electrolyte and microstructures determine the behavior of anodization. At various anodizing current regions and voltages different active-passive states are developed i.e., micro-arcing or sparking is often seen at higher voltages (above 50 V) and known as plasma electrolytic oxidation (PEO) or micro arc oxidation (MAO) [28-30]. MAO is considered as a substitute method for surface treatment because for magnesium alloys traditional anodization becomes uncertain as it did not lower the risk of premature fatigue failure which is not acceptable for engineering practices as fatigue strength plays an important role for load-bearing applications [31]. Number of studies shows that MAO on magnesium alloys concentrated on elevating anti-corrosion properties. Chen et al. applied polymer coatings over MAO treated AZ31 alloy then used nickel by electroless means and they proclaimed enhanced corrosion behavior [32]. Gnedenkov et al. utilized polytetrafluoroethylene over MAO layers in a scattered manner and reported decreased corrosion rate for magnesium alloys [33]. Simancas et al. analyzed different pretreatments with respect to protection against corrosion and proposed MAO for application of top-coat [34].

The aim of this research is to perform surface modification to protect magnesium and its alloys from corrosion in human body environments and finding the biocompatibility and effectiveness of Micro Arc Oxidation (MAO) at various electrolyte and voltages with further coating of fatty acids like stearic acid over Magnesium AZ31B alloy. The corrosion protection of these modified surfaces can be assessed through electrochemical techniques i.e., open circuit potential (OCP) and cyclic polarization (CP) potentiodynamic in simulated body fluid and temperature at different voltages. Scanning electron microscopy (SEM) and Energy-dispersive X-ray spectroscopy (EDX) will provide morphological characterization and elemental composition of materials, respectively.

Experimental Method

Material and Surface Preparation

The chemical composition of AZ31B magnesium alloy's is illustrated in Table 1. The sample of dimension 20×10×5 mm^2 was cut from the cylindrical rod of AZ3B and ground with SiC papers upto 3500 grit papers. The samples were then degreased with 70 vo.% solution of ethanol, then cleaned in de-ionized water by rinsing it time and stored in ethanol solution.

Table 1: Chemical composition of AZ31B magnesium alloy (wt.%).

Si	Fe	Cu	Mn	Al	Zn	Ni	Mg
0.023	0.0016	0.0031	0.35	2.95	1.11	0.009	Bal

Micro-Arc Oxidation Process

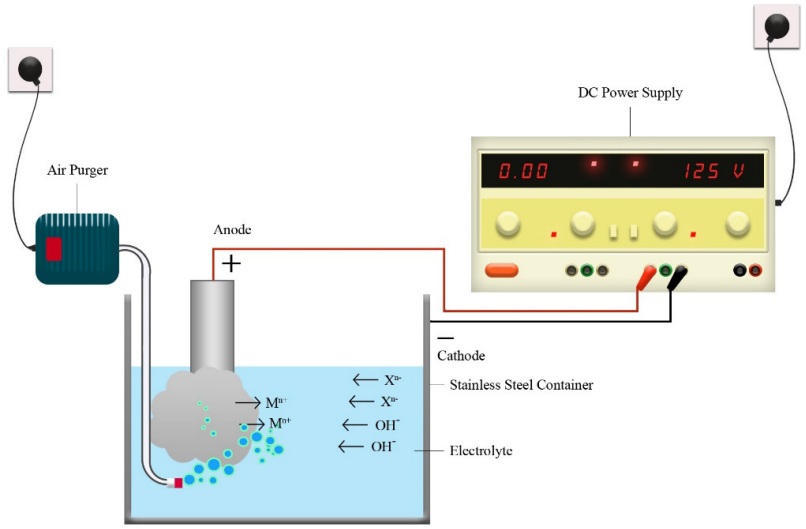

Figure 1: Schematic diagram of Micro-arc oxidation experimental setup.

The micro-arc oxidation electrolytic bath was prepared in de-ionized water by using the analytical grade chemicals of Merck with the composition illustrated in Table 2. The pH and conductivity of the electrolytic bath was 11.5 and 2.1 mS/cm respectively. The stainless steel 316L container was used as a cathode and high voltage was applied through specially designed DC power supply. The schematic diagram is shown in Figure 1.

Table 2: Composition of electrolytic bath of Micro Arc Oxidation.

Na_2SiO_3 (g-L^{-1})	NaF (g-L^{-1})	SDS* (g-L^{-1})	TiO_2 (g-L^{-1})	Borax (g-L^{-1})
20	10	0.05	30	5

* Sodium dodecyl sulfate (SDS)

Three voltages i.e., 125 V, 200 V and 250 V were applied on the surface of anode (AZ31B sample) for 10 minutes with continued air purging. The MAO samples were then cleaned in de-ionized water to remove residual salts several time and then stored in ethanol solution.

Characterization of MAO coating

The MAO samples were analyzed by stereomicroscope to check the smoothness or uniformity of the surface modification. The Scanning Electron Microscopy (SEM) and Elemental Dispersive Spectroscopy (EDS) for the morphology of MAO sample. The Open Circuit Potential (OCP) and Cyclic Polarization (CP) measurement to find the electrochemical behavior in simulated body fluid Ringer's Lactate solution at 37±1 °C. The hydrogen evolution behavior of the MAO samples was investigated by Potentio-dynamic Polarization (PDP) Test in simulated body fluid and to evaluate the corrosion rate. To find the pitting susceptibility in the MAO sample Cyclic Polarization (CP) was conducted.

Results and Discussion

Stereo microscopy

Figure 2 shows the stereomicrograph images before and after micro-arc oxidation (MAO) treatment on AZ31B magnesium alloy surface. The results show that MAO significantly change the morphology and topography of the magnesium alloy. As the voltages during the MAO changes, the uniformity as well as topography also changes. As in Figure 2 (b), when MAO was performed at 125 V a thin partial layer formed with precipitations on the surface of AZ31B sample. When the voltage was further increased to 200 V, a uniform layer thick layer was formed with constant immersion/exposure time. When the voltage increases to 250 V, the thick but non-uniform layer formed on the AZ31B sample with clusters of precipitates formed on the surface. The layers formed on the three samples were porous in nature and it was observed that porosity increases with the increase in the applied voltage.

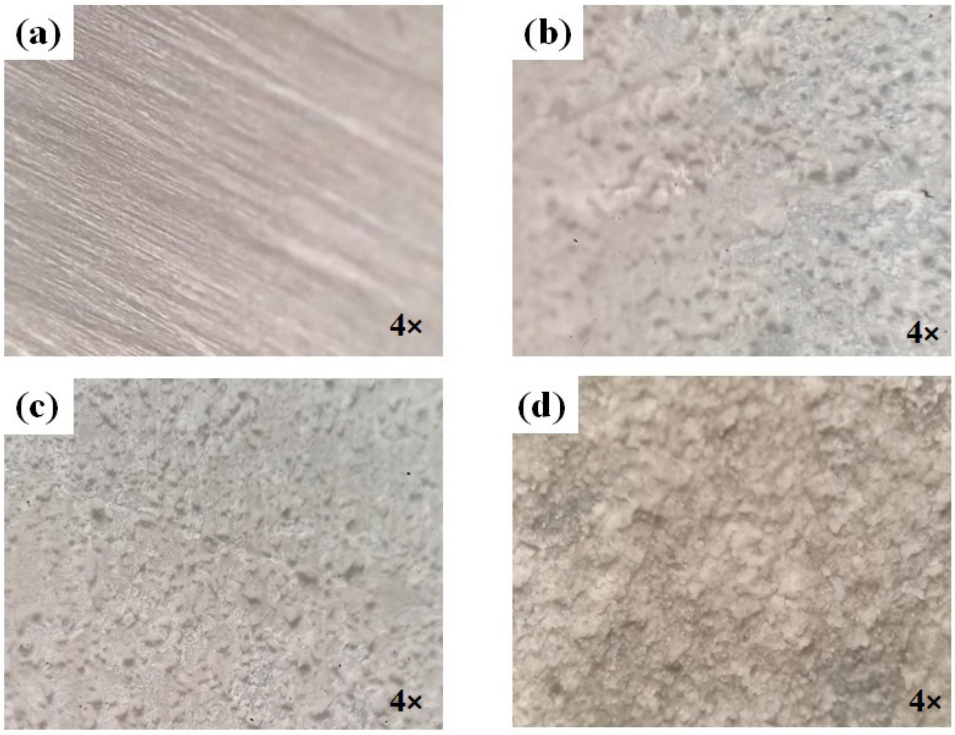

Figure 2: Stereomicrograph of AZ31B magnesium alloy (a) as received and after micro-arc oxidation (b) 125 V (c) 200 V (d) 250 V.

Scanning electron microscope

Figure 3 shows the SEM images after MAO treatment, on the AZ31B magnesium alloy with different applied voltage for constant immersion time. During MAO, many chimps and porosity formed on the surface of the oxide coating. The porosity is of different nature depending on the applied voltage. Due to the high voltage during MAO process, the sparking occurs on the AZ31B samples which formed sintered oxide coating with micro-pores. Those micro-probes entrapped the oxygen bubbles formed due to external air purging in the MAO electrolytic bath. Those entrapped oxygen bubbles increase the porosity in the MAO oxide coatings [35]. The mechanism of the MAO process explained with the help of schematic diagram in Figure 4.

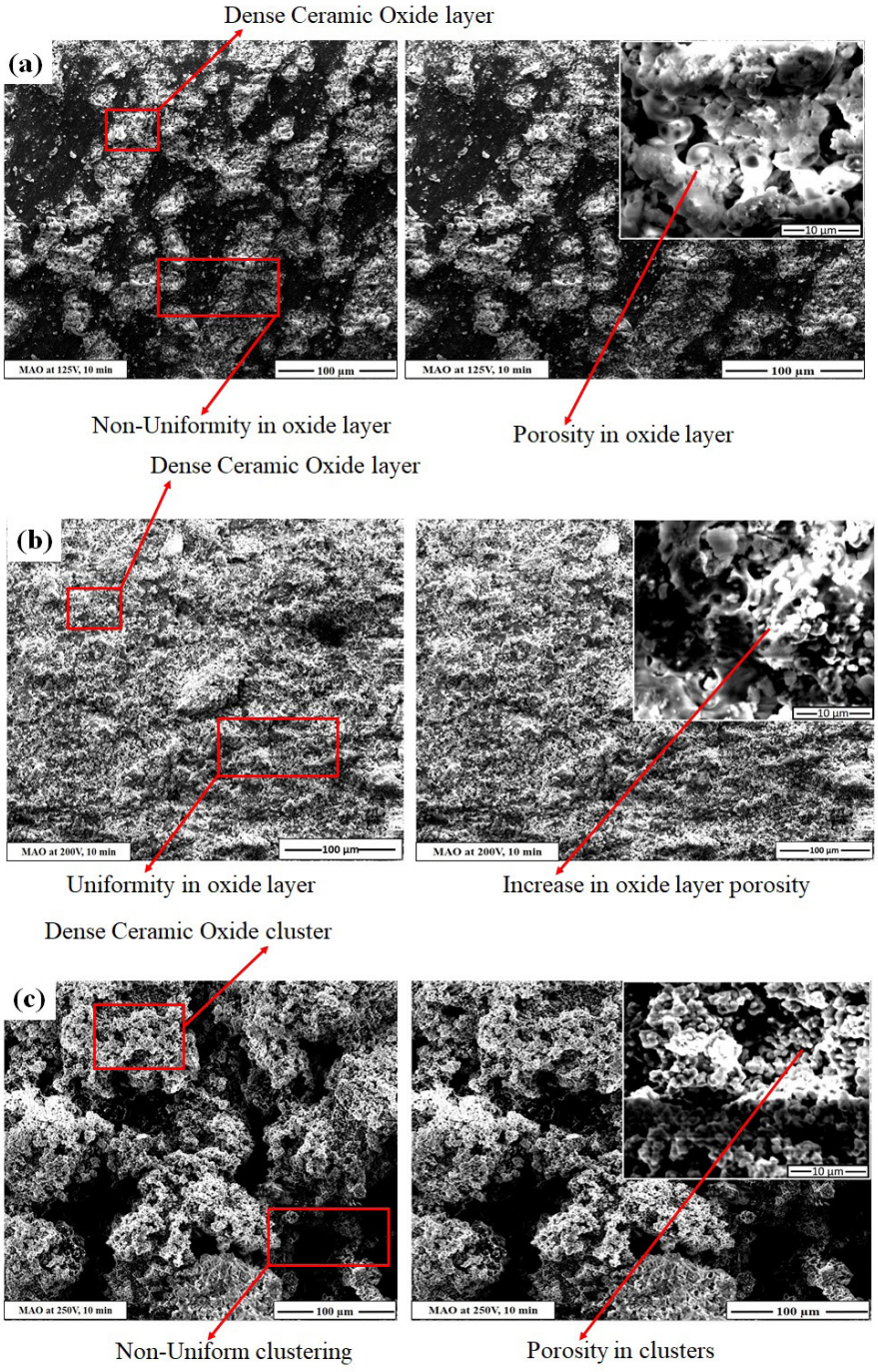

Figure 3: SEM photographs of AZ31B magnesium alloy after micro-arc oxidation (a) 125 V (b) 200 V (c) 250 V.

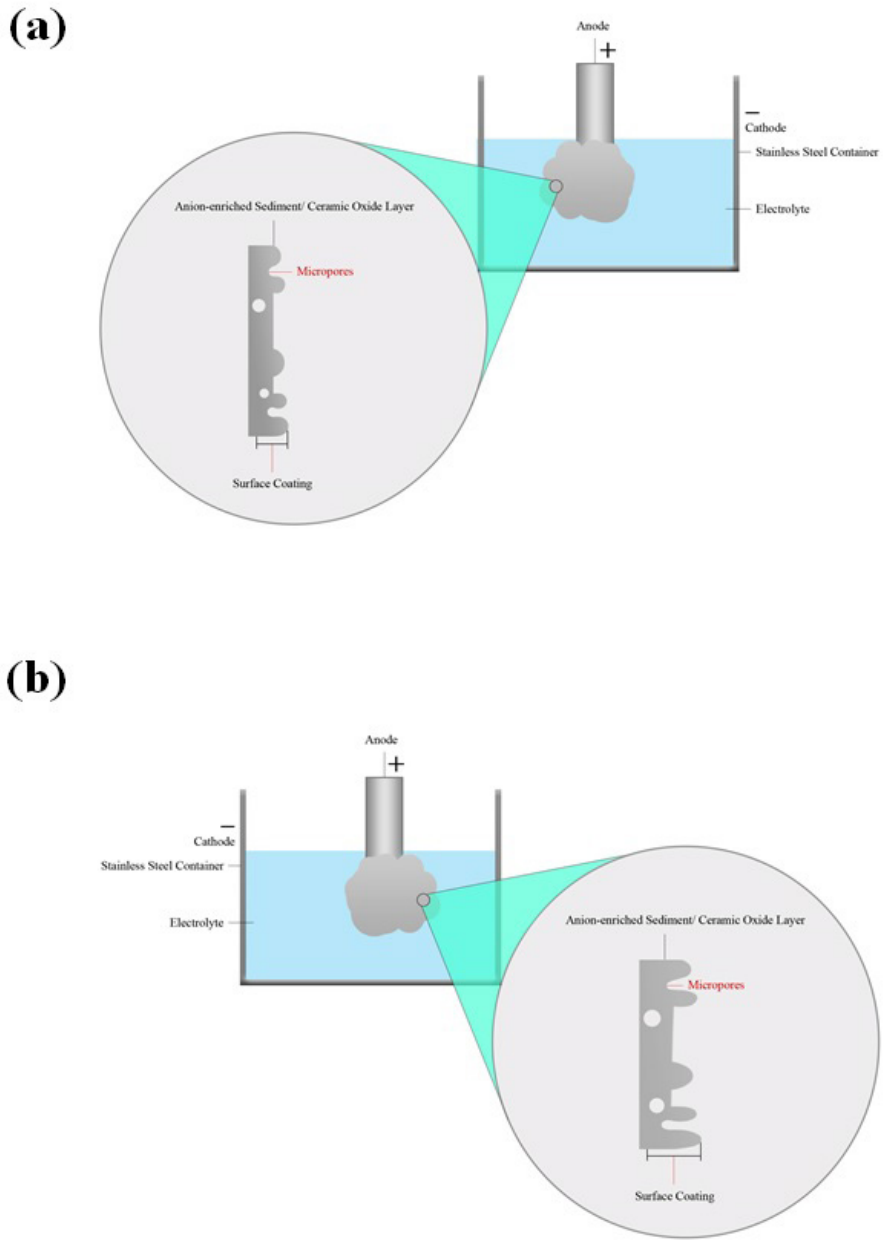

Figure 4: Schematic diagram of the formation of the oxide layer during Micro-Arc Oxidation process.

When the applied voltage was 125 V, non-homogenous oxide layer was developed as shown in Figure 4a. Partial oxide coating developed on the AZ31B sample, maximum surface area was unaffected. This is because for the certain composition of the electrolytic bath this was the low applied voltage. The oxide coating developed has pores and clusters of precipitation. The thickness of the oxide was ~ 6 to 8 µm. When the applied voltage increases to 200 V, the oxide coating develop has uniformity in it which support the fact that with the increase in the voltage homogeneity was developed on the AZ31B samples and also the oxide layer thickness increases to ~ 15 to 17 µm. With further increase in the applied voltage increases, the coating thickness of oxide layer increases to ~ 18 to 22 µm but again oxide layer become non-uniform. The cluster formed were large in size which decrease the contact with the surface.

Electrochemical Properties

Open circuit potential (OCP): Figure 5 shows the free potential or open circuit potential (OCP) of bare, and MAO treated AZ31B in the simulated body fluid i.e., Ringer's Lactate. The bare AZ31B has an OCP value of – 1.560 V vs Ag/AgCl, the potential remains stable after one hour in the Ringer's Lactate solution which shows that no side reaction or film formation on the bare sample during the testing. On MAO sample developed at 125 V applied voltage, the potential shifted towards more negative reduction value of – 1.592 V vs Ag/AgCl, which shows that due to MAO treatment the surface become more active and susceptible to more dissolution.

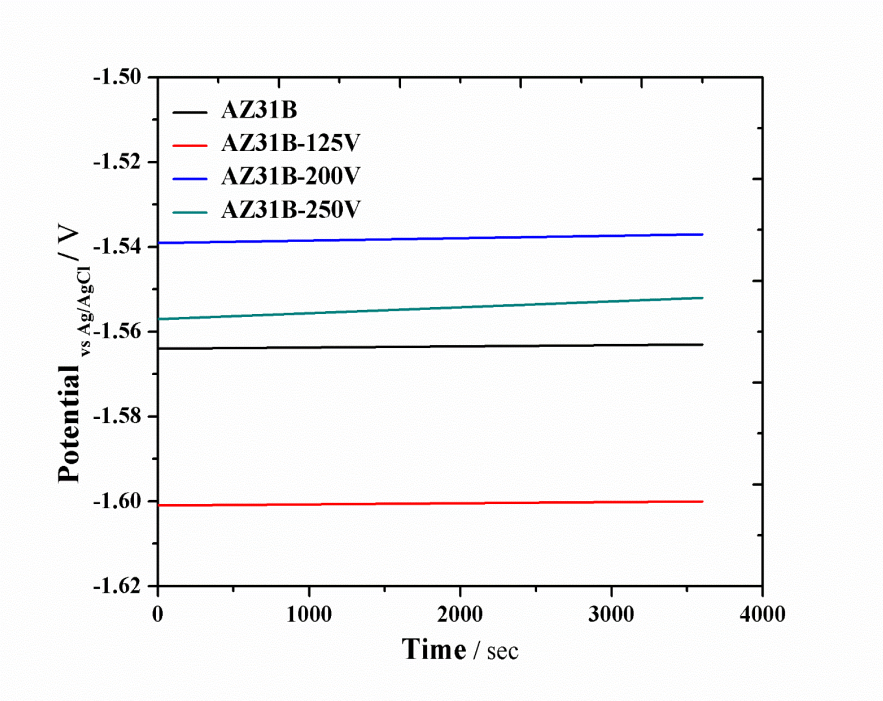

Figure 5: OCP trends of bare and MAO treated AZ31B magnesium alloy.

At 200 V, the potential shifted towards less negative reduction potential value of about – 1.539 V vs Ag/AgCl which was due to the uniform oxide formation. While at 250 V, the potential again shifted towards negative reduction potential value of about – 1.557 V vs Ag/AgCl.

Cyclic Polarization: Figure 6 shows the cyclic polarization curves of AZ31B before and after MAO treatment in Ringer Lactate solution. The kinetic parameters calculated from the Tafel fitting on the forward scan of the polarization curve are illustrated in Table 3. βa is the anodic slope, β_c is the cathodic slope, i_{corr} is the corrosion current density and E_{corr} is the corrosion potential. The increase in the β_a value reflects that less or slow kinetics of dissolution or anodic reaction. The β_a value of the bare AZ31B is 85.60 mV/decade which increases to 89.60 mV/decade after MAO at 125 V. With the increase in the MAO applied voltage to 200 V, the β_a value further increases to is 96.60 mV/decade which confirm that due to the MAO coating the dissolution or anodic reaction decreases. The decrease in the β_c value reflects that more or fast kinetics of deposition or cathodic reaction. After the MAO process, the AZ31B samples shows decreases in the β_c value confirms the fast reduction reaction on the surface.

Table 3: Kinetic parameters of bare and MAO treated AZ31B magnesium alloy.

Sample	Beta A (mV/dec)	Beta C (mV/dec)	i_{corr} (mA/cm^2)	E_{corr} (V)	Corrosion Rate (mpy)	Chi Squared × 10^{-12}
AZ31B	85.6	200.3	30.9	−1.34	26.62	612.3
AZ31B-125V	89.6	197.9	141	−1.51	121.4	910.7
AZ31B-200V	96.6	128.8	70.9	−1.47	61	514.5
AZ31B-250V	94.5	144.3	11.8	−1.34	10.18	230.5

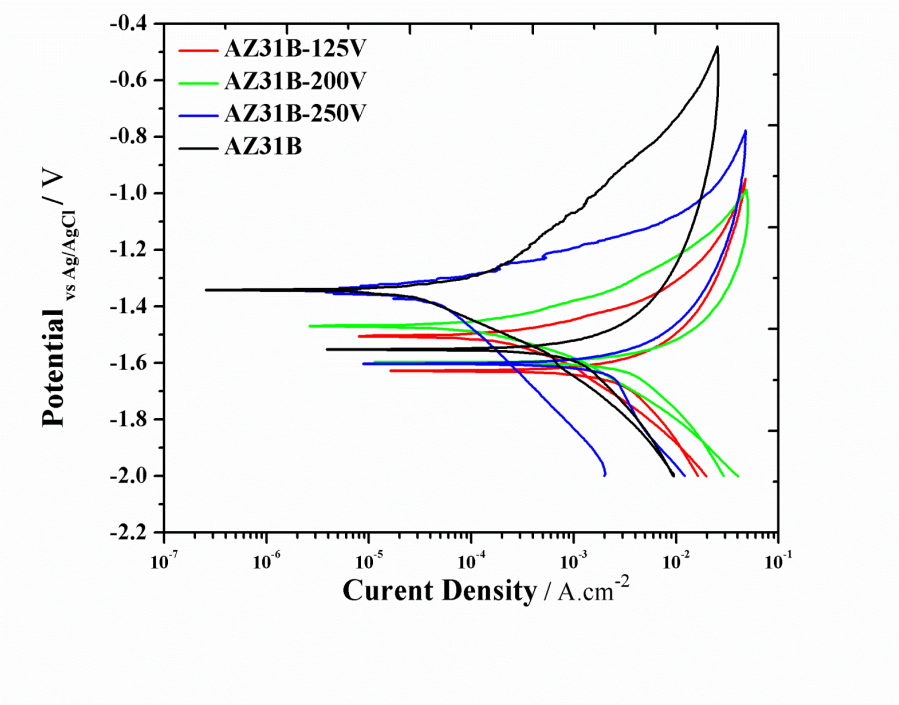

Figure 6: Cyclic Polarization curves of bare and MAO treated AZ31B magnesium alloy.

Conclusion

- With the increase in the voltage in the optimized electrolyte, the oxide layer thickness increases up to ~22 µm thickness.
- At high voltage of 250 V clusters formation of the ceramic oxide layer and porosity increases.
- The high voltage of 250 V shows improved corrosion resistance as compared to bare AZ31B substrate.

Acknowledgement

This research was funded by University of the Punjab, Lahore, Pakistan, grant number (2019-2121/TR).

Conflict of Interest

No conflict of interest.

References

1. Umer Masood Chaudry, Kotiba Hamad, Jung-Gu Kim (2020) A Further Improvement in the Room-Temperature Formability of Magnesium Alloy Sheets by Pre-Stretching. Materials 13(11): 2633.
2. Umer Masood Chaudry, Yeonju Noh, Gukin Han, Russlan Jaafreh, Tea-Sung Jun, et al. (2022) Effect of CaO on structure and properties of AZ61 magnesium alloy. Materials Science and Engineering: A 844: 143189.
3. Umer Masood Chaudry, Kotiba Hamad, Jung-Gu Kim (2020) Ca-induced Plasticity in Magnesium Alloy: EBSD Measurements and VPSC Calculations. Crystals 10(2): 67.
4. Umer Masood Chaudry, Ameeq Farooq, Kaab bin Tayyab, Abdul Malik, Muhammad Kamran, et al. (2022) Corrosion behavior of AZ31 magnesium alloy with calcium addition. Corrosion Science 199: 110205.
5. Gérrard Eddy Jai Poinern, Sridevi Brundavanam, Derek Fawcett (2012) Biomedical Magnesium Alloys: A Review of Material Properties, Surface Modifications and Potential as a Biodegradable Orthopaedic Implant. American Journal of Biomedical Engineering 2(6): 218-240.
6. R Zeng, W Dietzel, F Witte, N Hort, C Blawert (2008) Progress and Challenge for Magnesium Alloys as Biomaterials Advanced Biomaterials 10: B3-B14.
7. Zeng Rong-chang, Zhang Jin, Huang Wei-jiu, W Dietzel, KU Kainer, et al. (2006) Review of studies on corrosion of magnesium alloys. Transactions of Nonferrous Metals Society of China 16(Suppl 2): s763-s771.
8. Umer Masood Chaudry, Yeonju Noh, Kotiba Hamad, Tea-Sung Jun (2022) Effect of deformation temperature on the slip activity in pure Mg and AZX211. Journal of Materials Research and Technology 19: 3406-3420.
9. GUO Hui-xia, MA Ying, WANG Jing-song, WANG Yu-shun, DONG Hai-rong, et al. (2012) Corrosion behavior of micro-arc oxidation coating on AZ91D magnesium alloy in NaCl solutions with different concentrations. Transactions of Nonferrous Metals Society of China 22(7): 1786-1793.
10. F Witte, V Kaese, H Haferkamp, E Switzer, A Meyer-Lindenberg, CJ Wirth, et al. (2006) In vivo corrosion of four magnesium alloys and the associated bone response. Biomaterials 26(17): 3557-3563.
11. Sankalp Agarwal, James Curtin, Brendan Duffy, Swarna Jaiswal (2016) Biodegradable magnesium alloys for orthopaedic applications: A review on corrosion, biocompatibility and surface modifications. Mater Sci Eng C Mater Biol Appl 68: 948-963.
12. H Hornberger, S Virtanen, AR Boccaccini (2012) Biomedical coatings on magnesium alloys - a review. Acta Biomater 8: 2442-2455.
13. P Tian, X Liu, C Ding, (2015) In vitro degradation behavior and cytocompatibility of biodegradable AZ31 alloy with PEO/HT composite coating. Colloids and Surfaces B: Biointerfaces 128: 44-54.
14. A Alabbasi, M Bobby Kannan, R Walter, M Störmer, C Blawert (2013) Performance of pulsed constant current silicate-based PEO coating on pure magnesium in simulated body fluid. Materials Letters 106: 18-21.
15. Umer Masood Chaudry, Gukin Han, Yeonju Noh, Tea-Sung Jun (2023) Effect of Ca alloying and cryogenic temperature on the slip transmission

across the grain boundary in pure Mg. Journal of Alloys and Compounds 950: 169828.

16. GY Liu, J Hu, ZK Ding, C Wang (2011) Bioactive calcium phosphate coating formed on micro-arc oxidized magnesium by chemical deposition. Applied Surface Science 257(6): 2051-2057.

17. TF da Conceicão, N Scharnagl, W Dietzel, KU Kainer (2012) Controlled degradation of a magnesium alloy in simulated body fluid using hydrofluoric acid treatment followed by polyacrylonitrile coating. Corrosion Science 62: 83-89.

18. RIM Asri, WSW Harun, M Samykano, NAC Lah, SAC Ghani, et al. (2017) Corrosion and surface modification on biocompatible metals: A review. Mater Sci Eng C Mater Biol Appl 77: 1261-1274.

19. C García, S Ceré, A Durán (2006) Bioactive coatings deposited on titanium alloys. J Non-Cryst Solids 352: 3488-3495.

20. JJ Damborenea, N Pellegri, O de Sanctis, A Durán (1995) Electrochemical behaviour of SiO_2 sol-gel coatings on stainless steel. Journal of Sol-Gel Science and Technology 4: 239-244.

21. AR Phani, FJ Gammel, T Hack, H Haefke (2005) Enhanced corrosion resistance by sol-gel-based ZrO_2-CeO_2 coatings on magnesium alloys. Materials and Corrosion 56(2): 77-82.

22. M Zaharescu, L Predoana, A Barau, D Raps, F Gammel, et al. (2009) SiO2 based hybrid inorganic–organic films doped with TiO2–CeO2 nanoparticles for corrosion protection of AA2024 and Mg-AZ31B alloys. Corrosion Science 51(9): 1998-2005.

23. S Durdu, A Aytaç, M Usta (2011) Characterization and corrosion behavior of ceramic coating on magnesium by micro-arc oxidation. Journal of Alloys and Compounds 509(34): 8601-8606.

24. S Yagi, K Kuwabara, Y Fukuta, K Kubota, E Matsubara (2013) Formation of self-repairing anodized film on ACM522 magnesium alloy by plasma electrolytic oxidation. Corrosion Science 73: 188-195.

25. S Gaur, RK Singh Raman, AS Khanna (2014) In vitro investigation of biodegradable polymeric coating for corrosion resistance of Mg-6Zn-Ca alloy in simulated body fluid. Materials Science and Engineering C 42(9): 91-101.

26. F Gong, J Shen, R Gao, X Xie, X Luo (2016) Enhanced corrosion resistance of magnesium alloy by a silane-based solution treatment after an in-situ formation of the $Mg(OH)_2$ layer. Applied Surface Science 365: 268-274.

27. Chunmin Wang, Jun Shen, Xiankun Zhang, Bin Duan, Jiaxin Sang (2017) In vitro degradation and cytocompatibility of a silane/$Mg(OH)_2$ composite coating on AZ31 alloy by spin coating. Journal of Alloys and Compounds 714: 186-193.

28. Barbara Kazanski, Alexey Kossenko, Michael Zinigrad, Alex Lugovskoy (2013) Fluoride ions as modifiers of the oxide layer produced by plasmaelectrolytic oxidation on AZ91D magnesium alloy. Applied Surface Science 287 461-466.

29. Blawert C, Dietzel W, Ghali E, Song G (2006) Anodizing Treatments for Magnesium Alloys and Their Effect on Corrosion Resistance in Various Environments. Advanced Engineering Materials 8(6): 511-533.

30. A Ghasemi, VS Raja, C Blawert, W Dietzel, KU Kainer (2008) Processing-Microstructure Relationships in the Plasma Electrolytic Oxidation (PEO) Coating of a Magnesium Alloy. Surface and Coatings Technology 202: 3513-3518.

31. U Malayoglu, KC Tekin, S Shrestha (2010) Influence of post-treatment on the corrosion resistance of PEO coated AM50B and AM60B Mg alloys. Surface and Coatings Technology 205(6): 1793-1798.

32. AS Gnedenkov, SL Sinebryukhov, DV Mashtalyar, SV Gnedenkov (2013) Features of the corrosion processes development at the magnesium alloys surface. Surface and Coatings Technology 225: 112-118.

33. JN Li, P Cao, XN Zhang, SX Zhang, YH He (2010) J Mater Sci 22: 6038-6045.

34. LP Xu, A Yamamoto (2012) Characteristics and cytocompatibility of biodegradable polymer film on magnesium by spin coating. Colloids and Surfaces B: Biointerfaces 93: 67-74.

35. Allen Bai, Zhi-Jia Chen (2009) Effect of electrolyte additives on anti-corrosion ability of micro-arc oxide coatings formed on magnesium alloy AZ91D. Surface and Coatings Technology 203(14): 1956-1963.